Journal of Orthopaedic Translation 47 (2024) 235–248

Contents lists available at ScienceDirect

Journal of Orthopaedic Translation

journal homepage: www.journals.elsevier.com/journal-of-orthopaedic-translation

Original Article

Functionally improved mesenchymal stem cells via nanosecond pulsed electric fields for better treatment of osteoarthritis

Jianjing Lin [a,b,c,1], Kejia Li [d,e,1], Zhen Yang [a,b,1], Fuyang Cao [f], Liang Gao [g], Tong Ning [h], Dan Xing [a,b], Hui Zeng [i,*], Qiang Liu [a,b,**], Zigang Ge [d,***], Jianhao Lin [a,b,****]

[a] *Arthritis Clinical and Research Center, Peking University People's Hospital, No.11 Xizhimen South Street, Beijing, 100044, China*
[b] *Arthritis Institute, Peking University, Beijing, 100044, China*
[c] *Department of Sports Medicine and Rehabilitation, Peking University Shenzhen Hospital, Shenzhen, 518036, China*
[d] *Department of Biomedical Engineering, Institute of Future Technology, Peking University, Beijing, 100871, China*
[e] *Institute for Tissue Engineering and Regenerative Medicine, School of Biomedical Sciences, Faculty of Medicine, The Chinese University of Hong Kong, Shatin, Hong Kong Special Administrative Region of China*
[f] *Department of Orthopedics, Second Hospital of Shanxi Medical University, Taiyuan, 030001, China*
[g] *Department of Orthopaedics, The First Affiliated Hospital of Anhui Medical University, Hefei, 230041, China*
[h] *Institute of Medical Science, The Second Hospital, Cheeloo College of Medicine, Shandong University, Jinan, 250033, China*
[i] *Department of Orthopedics, the First Affiliated Hospital of Shenzhen University, Shenzhen Second People's Hospital, Shenzhen, 518035, China*

ARTICLE INFO

Keywords:
Cartilage
Extracellular vesicles
Mesenchymal stem cells
Nanosecond pulsed electric fields
Osteoarthritis

ABSTRACT

Background: Numerous approaches have been utilized to optimize mesenchymal stem cells (MSCs) performance in treating osteoarthritis (OA), however, the constrained diminished activity and chondrogenic differentiation capacity impede their therapeutic efficacy. Previous investigations have successfully shown that pretreatment with nanosecond pulsed electric fields (nsPEFs) significantly enhances the chondrogenic differentiation of MSCs. Therefore, this study aims to explore nsPEFs as a strategy to improve OA therapy by enhancing MSCs' activity and chondrogenic differentiation and also investigate its potential mechanism.

Methods: In this study, a million MSCs were carefully suspended within a 0.4-cm gap cuvette and subjected to five pulses of nsPEFs (100 ns at 10 kV/cm, 1 Hz), with a 1-s interval between each pulse. A control group of MSCs was maintained without nsPEFs treatment for comparative analysis. nsPEFs were applied to regulate the MSCs performance and hinder OA progresses. In order to further explore the corresponding mechanism, we examined the changes of MSCs transcriptome after nsPEF pretreatment. Finally, we studied the properties of extracellular vesicles (EVs) secreted by MSCs affected by nsPEF and the therapeutic effect on OA.

Results: We found that nsPEFs pretreatment promoted MSCs migration and viability, particularly enhancing their viability temporarily *in vivo*, which is also confirmed by mRNA sequencing analysis. It also significantly inhibited the development of OA-like chondrocytes *in vitro* and prevented OA progression in rat models. Additionally, we discovered that nsPEFs pretreatment reprogrammed MSC performance by enhancing EVs production (5.77 ± 0.92 folds), and consequently optimizing their therapeutic potential.

Conclusions: In conclusion, nsPEFs pretreatment provides a simple and effective strategy for improving the MSCs performance and the therapeutic effects of MSCs for OA. EVs-nsPEFs may serve as a potent therapeutic material for OA and hold promise for future clinical applications.

The translational potential of this article: This study indicates that MSCs pretreated by nsPEFs greatly inhibited the development of OA. nsPEFs pretreatment will be a promising and effective method to optimize the therapeutic effect of MSCs in the future.

* Corresponding author. Department of Orthopedics, the First Affiliated Hospital of Shenzhen University, Shenzhen Second People's Hospital, Shenzhen, 518035, China.
** Corresponding author. Arthritis Clinical and Research Center, Peking University People's Hospital, No.11 Xizhimen South Street, Beijing, 100044, China.
*** Corresponding author. Department of Biomedical Engineering, Institute of Future Technology, Peking University, Beijing, 100871, China.
**** Corresponding author. Arthritis Clinical and Research Center, Peking University People's Hospital, No.11 Xizhimen South Street, Beijing, 100044, China.
E-mail addresses: zenghui_36@163.com (H. Zeng), liuqiang_pku@126.com (Q. Liu), gez@pku.edu.cn (Z. Ge), linjianhao@pkuph.edu.cn (J. Lin).
[1] These authors contributed equally to this work.

https://doi.org/10.1016/j.jot.2024.03.006
Received 4 January 2024; Received in revised form 25 February 2024; Accepted 21 March 2024
Available online 5 July 2024

1. Introduction

Osteoarthritis (OA) is one of the most common reasons of joint pain and disability, which seriously affects a hundred million people's daily lives [1,2]. Cell therapy is considered to be an innovative and promising therapy for OA, in which, mesenchymal stem cells (MSCs) have been popularly studied because of their immunosuppressive activity, multilineage potential, significant paracrine activity and a simple growth process *in vitro* [3–5]. To obtain the sufficient cellular quantity, MSCs need to be expanded *in vitro*. However, the proliferation ability and other superior performance of MSCs gradually declines with its expansion, and is negatively correlated with the age of the MSCs donors [6], which increases the cost of time and money, and greatly affects the therapeutic effect of OA [7]. MSC-derived EVs have been reported to suppressing the inflammatory immune microenvironment and alleviate pain in OA patients [8,9].

Many methods are applied to enhance therapeutic potency of MSCs for OA. MSCs pretreated with Vitamin E for 24 h significantly impeded the progression of OA [10]. 3D aggregate culture augmented the paracrine functions of MSCs, and prevent cartilage degradation of OA mouse [11]. Low-intensity pulsed ultrasound treatment for a few days promoted the migration, proliferation and differentiation ability of MSCs and hinder the onset and progression of TMJ-OA [12]. Nevertheless, these methods still have some disadvantages for single target or complex operation or long processing time. There is still a need for the efficient, fast, and multi-targeted methods to improve the therapeutic potency of MSCs for OA [13].

Pulsed electric fields (PEFs) are one of the important biophysical signals. With certain parameters, PEFs can significantly affect cell phenotype, regulate stem cells differentiation, and incur comprehensive biological effects. Such as PEFs can activate calcium ion-related signal pathways, and significantly promote the osteogenic and chondrogenic differentiation of MSCs [14]. Nanosecond pulsed electric fields (nsPEFs), a novel technology with relatively short duration (nanoseconds, ns) and subsequent high voltages (up to kV/cm), have been reported to have the modulation effects on stem cells. Previously, our research group found that nsPEFs can affect the phenotype of chondrocytes by regulating the Wnt/β-catenin signaling pathway [15]. Besides, we found that pretreatment of nsPEFs (100 ns, 10 kV/cm, 1 Hz, 5 pulses) can enhance the trilineage differentiation potential of MSCs [16] and enhanced osteochondral defect repair *in vivo* [17,18]. Especially, the nsPEFs pretreatment can be finished in 10 s before cell therapy. These findings prompt us to conduct more research on the regulation of MSCs by nsPEFs, and explore whether nsPEFs pretreatment can improve therapeutic potency of MSCs for more complex joint diseases and OA.

We aimed to investigate the impact of nsPEFs pretreatment on the migration and viability of MSCs, building upon our earlier findings that nsPEFs can stimulate MSC chondrogenic differentiation. Furthermore, we sought to evaluate the therapeutic effects of nsPEF-pretreated MSCs through *in vitro* co-culture with IL-1β-induced OA-like chondrocytes and *in vivo* joint injection into anterior cruciate ligament transection (ACLT)-induced Sprague Dawley rat OA models. Additionally, we employed RNA-seq analysis to examine the regulatory effects of nsPEFs on MSCs. Finally, we also detect MSC-derived EVs to explore the potential mechanism of nsPEFs pretreated-MSCs on OA treatment. Our hypothesis is that nsPEFs can potentially enhance the release, performance, and therapeutic potential of MSC-derived EVs to treat OA.

2. Materials and methods

2.1. Cell isolation and culture

All animal experiments were approved by the Institutional Animal Care and Use Committee of Peking University (COE-GeZ-7). Rat bone marrow mesenchymal stem cells (rMSCs) and chondrocytes were harvested from 8-week-old Sprague Dawley (SD) rats according to our previous study [19]. Human bone marrow mesenchymal stem cells (hMSCs) were obtained from OA patients undergoing total knee arthroplasty. All procedures were in accordance with the Helsinki Declaration and informed consent of the patients was obtained. The study was approved by the Ethics Review Committee of Peking University People's Hospital (2018PHC061). The cells were cultured in Dulbecco's modified Eagle's medium (DMEM, Hyclone) supplemented with 10% fetal bovine serum (FBS, Gibico) and 1% penicillin/streptomycin (PS, Amresco). Cultures were maintained at 37 °C in humidified atmosphere with 5% CO2. The cultured medium was changed every three days. MSCs at passage 5 and chondrocytes at passage 3 were used for subsequent experiments.

2.2. Characteristics of MSCs

MSCs at passage 5 were detected using the BD FACSCelesta flow cytometer (Becton Dickinson, Franklin Lakes, NJ, USA) to identify the MSCs surface markers CD29, CD44, CD90 and CD105 and the negative markers CD34 and CD45. The data were analysed using the FlowJo software.

For osteogenic and adipogenic differentiation, the MSCs were cultured with osteogenic induction medium and adipogenic induction medium at 37 °C in humidified atmosphere with 5% CO2, respectively. After 14 days, cell cultures were stained with Alizarin Red (for osteogenic induction) and Oil Red O (for adipogenic induction) according to our previous study [16]. For chondrogenic differentiation, MSCs pellets (2.5 × 105 cells) were cultured with chondrogenic induction medium in a 3-dimensional pellet culture model [18]. After 14 days, cell pellets were frozen, sectioned at 8 μm and stained with Alcian Blue.

2.3. Application of nsPEFs

The nsPEFs generator was applied according to the approach described previously [20]. Previous study found Tca8113 cells showing early apoptosis after nsPEFs (60 ns, 20 kV/cm, 1 Hz, 20 pulses) combining with radiotherapy [21]. Zhang found that pretreatment of nsPEFs (100 ns, 10 kV/cm or 20 kV/cm, 1 Hz, 5 pulses) can enhance proliferation of chondrocyte [15]. So we think 5 pulses are safe for cells. We previously found that nsPEFs (100 ns, 10 kV/cm, 1 Hz, 5 pulses) can improve the stemness of porcine bone marrow MSCs (pMSCs), hMSCs and rMSCs, and promote the osteochondral defect repair of rats [16,18,22]. In this study, nsPEFs with the same parameters were still applied to regulate the MSCs performance. As previously described [16,18], one million MSCs were suspended in 1 mL DMEM within 0.4-cm gap cuvette (Bio-Rad, 165–2088, USA) and stimulated by 5 pulses of nsPEFs (100 ns at 10 kV/cm, 1 Hz), the time interval between two pulses was 1 s with an overall nsPEFs processing time of 10 s. Throughout the process, the cells remain dispersed throughout the solution, evenly exposed to electrical stimulation. MSCs without nsPEFs treatment served as control.

2.4. Cell Counting Kit-8 (CCK-8) analysis of MSCs

Viability of MSCs with or without nsPEFs pretreatment was evaluated with Cell Counting Kit-8 (CA1210, Solarbio) at days 1, 3 and 7 after nsPEF treatment. 10 μL CCK-8 solution were added to each well of 96-well plates and incubated for 2 h. The absorbance was measured at a wavelength of 450 nm using the Microplate Reader (680, Bio-Rad). Five samples from each group were measured.

2.5. Migration analysis of MSCs

For transwell migration assay, MSCs with or without nsPEFs pretreatment in serum-free DMEM medium were inoculated in the 8 μm pore size upper layer (Corning, USA) of the 24-well transwell chamber. The lower layer contained DMEM medium with 10% FBS. After 24 h incubation, the upper chamber was fixed with 4% paraformaldehyde for

15 min and stained with crystal violet staining solution for 15 min. After washing with PBS, the upper surface of the transwell chamber was swabbed to remove the cells that did not move to the lower surface. Finally, the cell migration of each group was examined by microscope by counting the cell numbers in the lower surface of the upper chamber. Four samples from each group were measured.

For the scratch, MSCs with or without nsPEFs pretreatment were cultured on a 12-well plate and cultured to confluence. Sterile pipette tip (200 μL) was used to make a scratch on the cell layer. The closure of the scratch over time reflects the migratory capacity of MSCs. Images of the scratch area were captured at 0 h, 12 h and 24 h, and the extent of scratch closure was measured using image analysis software. Four samples from each group were measured.

2.6. Chondrogenic differentiation of MSCs

MSCs with or without nsPEFs pretreatment pellets (2.5×10^5 cells) were induced by chondrogenic induction medium, medium was refreshed every 3 days. After 14 days, pellets were harvested for haematoxylin and eosin (H&E), Safranin O, Toluidine Blue staning and collagen type II immunohistochemistry staining and chondrogenic gene anallysis.

2.7. Gene expression analysis

Total RNA was extracted from pellets or chondrocytes under each culture condition with TRIzol Reagent (DP424, Tiangen) according to the manufacturer's protocol. Total RNA was quantified with a Nanodrop spectrophotometer (ND-1000, Thermo), and 2 μg RNA were reverse transcribed with FastQuant RT Kit (KR106, Tiangen) in a PCR thermal cycler (Mycycler, Bio-Rad). Quantitative RT-PCR (qRT-PCR) was performed in the PCR system (Pikoreal 96, Thermo) with Real Master Mix SYBR Green (FP202, Tiangen) according to the manufacturer's protocols. The primer sequences are listed in Table S1 in Supporting Information. Each qPCR test was performed on four different experimental samples with three technical replicates, and the representative results are displayed as target gene expression normalized to glyceraldehyde-3-phosphate dehydrogenase (GAPDH) gene. Relative expression of each gene was expressed as fold changes by the $2-\Delta\Delta Ct$ method.

2.8. Co-culture of chondrocytes and MSCs

Chondrocytes were seeded in a 24-well culture plate containing 1 mL of proliferation medium. At 80% confluence, OA-like chondrocytes were induced by 10 ng/mL IL-1β (Peprotech) for 24 h. For the co-culture, rMSCs (1×10^4 cells) with or without nsPEFs pretreatment (100 ns, 10 kV/cm, 1 Hz, 5 pulses) were cultured in the upper layer of the transwell chamber (0.4 μm, 24-well, Corning). All cells were cultured in DMEM medium containing 10% FBS and 1% PS.

2.9. Cellular immunofluorescence

After 24 h co-culture, immunofluorescence staining was utilized to confirm the expression of CollagenII and MMP13 proteins in chondrocytes. Chondrocytes were washed with PBS and fixed with 4% paraformaldehyde for 15 min and then washed twice with PBS. The cells were then permeabilized with 0.5% Triton X-100 for 15 min, followed by blocking with 5% bovine serum albumin (BSA) for 1 h, prior to being incubated with primary antibodies against CollagenII (1:100, AF0135, Affinity) or MMP13 (1:100, AF5355, Affinity) overnight. After washing off the primary antibodies, the cells were incubated with CoraLite488 conjugated Affinipure goat anti-rabbit IgG (1:500, SA00013-2, Proteintech) secondary antibodies at room temperature for 1 h. The cell nuclei were stained with DAPI (D9542, Sigma–Aldrich) for 5 min. The chondrocytes were then imaged of randomly selected areas by fluorescence microscope (ThermoFisher, USA).

2.10. MSCs tracking in vivo

For deep tracking of the long-term retention of rMSCs in the rat joint cavity, rMSCs were stained with DiR dye (mb12482-1, Meilunbio, China) according to the manufacturer's protocol. DiR-rMSCs (1×10^6 cells) with or without nsPEFs pretreatment suspended in 100 μl PBS were injected into the knee joint cavity of the right hind leg of the rat (8 weeks old, n = 5/group). Rats under isoflurane anesthesia were observed using an IVIS 200 optical imaging system (Xenogen, Caliper Life Sciences) on days 0, 1, 3, 5, 7, 14, and 21, respectively. Under the condition that the excitation wavelength is 740 nm and the emission wavelength is 790 nm, the region of interest (ROI) at the knee joint was selected, and the radiation efficiency was calculated in the region of interest. Living Image 4.5.5 software (Perkin Elmer) was used to obtain and analyze the luminescence images of the joint cavity of DiR-rMSC and DiR-rMSC-nsPEFs.

2.11. Animal experiment

The animal experiments were approved by the Institutional Animal Care and Use Committee of Peking University (COE-GeZ-7). 8-week-old male Sprague Dawley (SD) rats were anesthetized with animal isoflurane anesthesia machine (R520, RWD Life Science), for 4% isoflurane induction, 1.5% isoflurane maintenance. Anterior cruciate ligament transection (ACLT) was operated to produce the OA change of the right knee of rats. A total of 48 rats were randomly divided into four groups (6 rats per group) as follows: normal group (without any treatment); PBS group (OA modle, PBS injection); rMSCs group (OA modle, rMSCs injection); rMSC-nsPEFs group (OA modle, nsPEFs-pretreatment rMSCs injection). 2 weeks after surgery, cell therapy was performed, for which, 100 μl PBS or MSCs suspended in 100 μl PBS was injected to joint cavity-right knee two times at two weeks interval. 48 rats (n = 6/group) were sacrificed at the 4th and the 12th weeks after the first joint injection.

2.12. Gait analysis

Rat gaits were measured before surgery, day 1, 7 and 14 after surgery, and 1, 2, 4, 8, 12 weeks after the first joint injection using the Catwalk apparatus (Noldus, Wageningen, Netherlands). During the test, each rat was individually placed on the glass path and successfully walked from one end to the other (n = 6/group). The paw prints of rats were reflected by LED light which was emitted from the glass plate and then detected by the high-speed video camera that was positioned under the glass walkway. The gait data (Print area, Mean intensity, Swing speed and Duty cycle) were collected by Catwalk software XT 10.6 (Noldus).

2.13. Microcomputed tomography (micro-CT) analysis

At week 4 and 12 post-treatment, the knee joint samples were fixed in 4% paraformaldehyde for 24 h and then scanned by micro-CT (n = 6/group). The 3D reconstructed images were evaluated and the subchondral bone (diameter = 2 mm, thickness = 0.5–0.8 mm) of medial tibial plateau was assigned as the region of interest (ROI). The subchondral bone changes were estimated based on the Bone volume/total tissue volume (BV/TV), trabecular thickness (Tb.Th), trabecular separation (Tb.Sp) and trabecular number (Tb.N).

2.14. Histology and immunohistochemical analysis of knee joint

After the micro-CT scan, the knee joint samples were decalcified in EDTA, then embedded in paraffin after dehydration in a gradient alcohol. The embedded specimens were cut into 3 μm thick sagittal sections and analyzed by Safranin-O & fast green and immunohistochemical staining (Collagen II (1: 400; ab34712, Abcam) or MMP13 (1: 500; PA5-27242, ThermoFisher)). The severity of cartilage degeneration

was evaluated using Mankin scoring system (Table S2 in Supporting Information, n = 6/group).

2.15. RNA sequencing

After 2 h of stimulation with or without nsPEFs, total RNA of rMSCs was extracted using Trizol Reagent (DP424, Tiangen) following the manufacturer's protocol. RNA-seq was conducted by Shanghai Biotechnology Corporation (Shanghai, China). Gene expression level was quantified using DEGseq [23]. The genes with counts greater than 10, at least two-fold change in expression, and p value less than 0.05 were considered to be differentially expressed. GO and KEGG enrichment were performed by Metascape [24] and KOBAS [25], respectively. Three samples from each group were measured.

2.16. Isolation of extracellular vesicles (EVs)

After pretreating with nsPEFs, rMSCs were inoculated in DMEM medium with 1% PS and 10% FBS and in which EVs were removed by centrifuged at 100,000 g for 18 h. 24 h later, cell culture supernatant was collected. In order to remove dead cells and cell debris, the supernatants were centrifuged at 300 g for 10 min, 2000 g for 10 min and 10,000 g for 30 min at 4 °C. Next, the supernatants were transferred to a fresh ultracentrifuge tube and centrifuged at the speed of 100,000 g (CP100NX, HITACHI, Japan) for 70 min at 4 °C. Then, the pellets were resuspended with PBS in each tube. EVs were obtained after be centrifuged at 100,000 g for 70 min at 4 °C and resuspended with cold PBS.

2.17. Transmission electron microscopy (TEM)

10 μL EV suspension solution were loaded on the carbon-coated 200 mesh cupper grid and stained with 2% phosphotungstanic acid on the surface of the grid for 2 min. Subsequently, the excess solution on the grid was removed by filter paper and dried at room temperature. EVs were observed under a JEM-1400 transmission electron microscope (JEOL, Tokyo, Japan).

2.18. Nanoparticle tracking analysis (NTA)

The concentration and particle size distribution of the EVs were determined by nanoparticle tracking analysis (NTA) using a NanoSight NS300 system (Malvern Instruments, Malvern, UK). EVs samples were diluted in PBS (HyClone) and injected into the instrument at a constant flow through a 1 mL syringe. When the particle concentration was kept within the optimal detection range, the movement video was captured for 60 s in triplicate and the temperature was maintained automatically at 22 °C. A standard detection threshold of 3 and a camera sensitivity level of 14 were set in all measurements. The videos were subsequently analyzed with NTA software 2.3 based on Brownian motion.

2.19. Western blotting

According to the manufacturer's instructions, EVs Protein lysate concentrations were determined using a Pierce BCA Protein Assay Kit (Solarbio, China). An appropriate amount of sodium dodecyl sulfate (SDS) buffer (Solarbio, China) was added and mixed, and protein electrophoresis was performed after denaturation in 95 °C water for 10 min. Proteins were separated by sodium dodecyl sulfate-polyacrylamide gel electrophoresis and transferred onto polyvinylidene fluoride membrane. After blocking with 5% bovine serum albumin (BSA) blocking solution for 1 h at room temperature, membranes were incubated with anti-CD9 primary antibody (1: 1000; Affinity, AF5139, China), ALIX (1: 2000; Proteintech, 12422-1 -AP, USA), TSG101 (1:500; Affinity, DF8427, China) and Calnexin (1:1000; Affinity, AF5362, China) at 4 °C overnight, respectively. After incubating with anti-rabbit IgG, HRP-linked Antibody (1: 2000; CST, 7074s, USA) for 1 h at room temperature, protein bands were detected with ChemiDoc XRS 1 Molecular Imager (Bio-Rad), and quantificated with the ImageJ software.

2.20. Uptake of EVs by chondrocytes

For the fluorescent labeling of EVs, Dil solution (C1036, Beyotime) was added to PBS and incubated according to the procedure recommended by the manufacturer. Excess Dil dye was removed by ultracentrifugation at 100,000×*g* for 70 min at 4 °C. EVs was washed twice with PBS and resuspended. These Dil-labeled EVs and EVs-nsPEFs (1×10^9 particles/mL) were co-cultured with chondrocytes for 6 h, 12 h, and 24 h, rinsed with PBS, and fixed in 4% paraformaldehyde. The cell nuclei were stained with DAPI (D9542, Sigma–Aldrich) for 5 min. The chondrocytes were then imaged of randomly selected areas by fluorescence microscope (ThermoFisher, USA).

2.21. Cell Counting Kit-8 (CCK-8) analysis of chondrocytes

Viability of chondrocytes co-cultured with EVs and EVs-nsPEFs (1×10^9 particles/mL) was evaluated with Cell Counting Kit-8 (CA1210, Solarbio) at days 1, 3 and 7. 10 μL CCK-8 solution were added to each well of 96-well plates and incubated for 2 h. The absorbance was measured at a wavelength of 450 nm using the Microplate Reader (680, Bio-Rad). Five samples from each group were measured.

2.22. 5-Ethynyl-2′-deoxyuridine (EDU) analysis of chondrocytes

Chondrocytes proliferation was evaluated using an EDU kit (C10310-3, RIBOBIO) in accordance with the manufacturer's protocol. Chondrocytes were seeded onto a 96-well plate at the concentration of 1×10^3 cells/well and cultured for 2 h with EDU (50 μM). Chondrocytes were washed with PBS and fixed with 4% paraformaldehyde for 15 min and then washed twice with PBS. The cells were then permeabilized with 0.5% Triton X-100 for 15 min, followed by 100 μL of Apollp reaction mixture was added for 30 min. The cell nuclei were stained with DAPI (D9542, Sigma–Aldrich) for 5 min. The chondrocytes were then imaged of randomly selected areas by fluorescence microscope (ThermoFisher, USA).

2.23. Migration analysis of chondrocytes

For transwell migration assay, chondrocytes co-cultured with EVs and EVs-nsPEFs (10^9 particles/mL) in serum-free DMEM medium were inoculated in the 8 μm pore size upper layer (Corning, USA) of the 24-well transwell chamber. The lower layer contained DMEM medium with 10% FBS. After 24 h incubation, the upper chamber was fixed with 4% paraformaldehyde for 15 min and stained with crystal violet staining solution for 15 min. After washing with PBS, the upper surface of the transwell chamber was swabbed to remove the cells that did not move to the lower surface. Finally, the cell migration of each group was examined by microscope by counting the cell numbers in the lower surface of the upper chamber. Four samples from each group were measured.

2.24. Statistical analysis

Results were presented as the mean ± SD and normalized to the control group. Student's test and ANOVA was carried out with the least significant difference (LSD) using Prism 8.21 software (GraphPad). The statistical significance level was set as $P < 0.05$.

3. Results

3.1. Pretreatment with nsPEFs enhanced chondrogenic differentiation, migration, and viability of MSCs

The cultured rMSCs and hMSCs showed a uniform and elongated

spindle shape, with a typical spiral arrangement (Fig.S1A in Supporting Information). The results of Alizarin Red, Oil Red O and Alcian Blue staining showed that rMSCs and hMSCs had multidirectional differentiation potentials (Fig.S1B in Supporting Information). The cell surface antigen phenotype of rMSCs and hMSCs was assessed by flow cytometry. rMSCs expressed high levels of CD29 (98.9%), and CD90 (98.4%), and were negative for expression of CD34 (1.08%) and CD45 (0.095%). HMSCs expressed high levels of CD44 (98.7%), and CD105 (95%), and were negative for expression of CD34 (0.5%) and CD45 (0.32%) (Fig. S1C in Supporting Information).

Firstly, we investigated the effect of nsPEFs on the proliferation of MSCs (Fig. 1). The results showed that nsPEF treatments significantly promoted the viability of rMSCs (1.2 folds at day 1, 1.2 folds at day 3 and 1.2 folds at day 7, Fig. 1A), while the effect on the viability of hMSCs appeared at 7 days after nsPEFs pretreatment (1.9 folds, Fig.S2A). The migration of rMSCs and hMSCs were detected after pretreatment with nsPEFs. Transwell assay showed that the number of MSCs that migrated with nsPEFs pretreatment is 2.2- and 2.3-fold higher than control group (Fig. 1B, C and Fig.S2B, C in Supporting Information). MSCs pretreated with nsPEFs (MSCs-nsPEFs) in the scratch assay showed enhanced migration with accelerated gap closure of the cell-free area compared with the wild-type MSCs at 12 h and 24 h, especially after nsPEFs treatment for 24 h, the gap closure of rMSCs and hMSCs was completely closed (Fig. 1D, E and Fig.S2D, E in Supporting Information). These data indicate that nsPEFs can enhance the mobility of rMSCs and hMSCs.

In order to confirm the effect of nsPEFs on the chondrogenic differentiation of MSCs, the pellets were analyzed after 14 days of pellet culture. Pellet staining was significantly enhanced in the rMSC-nsPEFs group. Simultaneously, nsPEFs could enhance the chondrogenic gene expression of *Sox9 (3.1 folds)*, *Col2 (2.6 folds)* and *Acan (1.8 folds)*

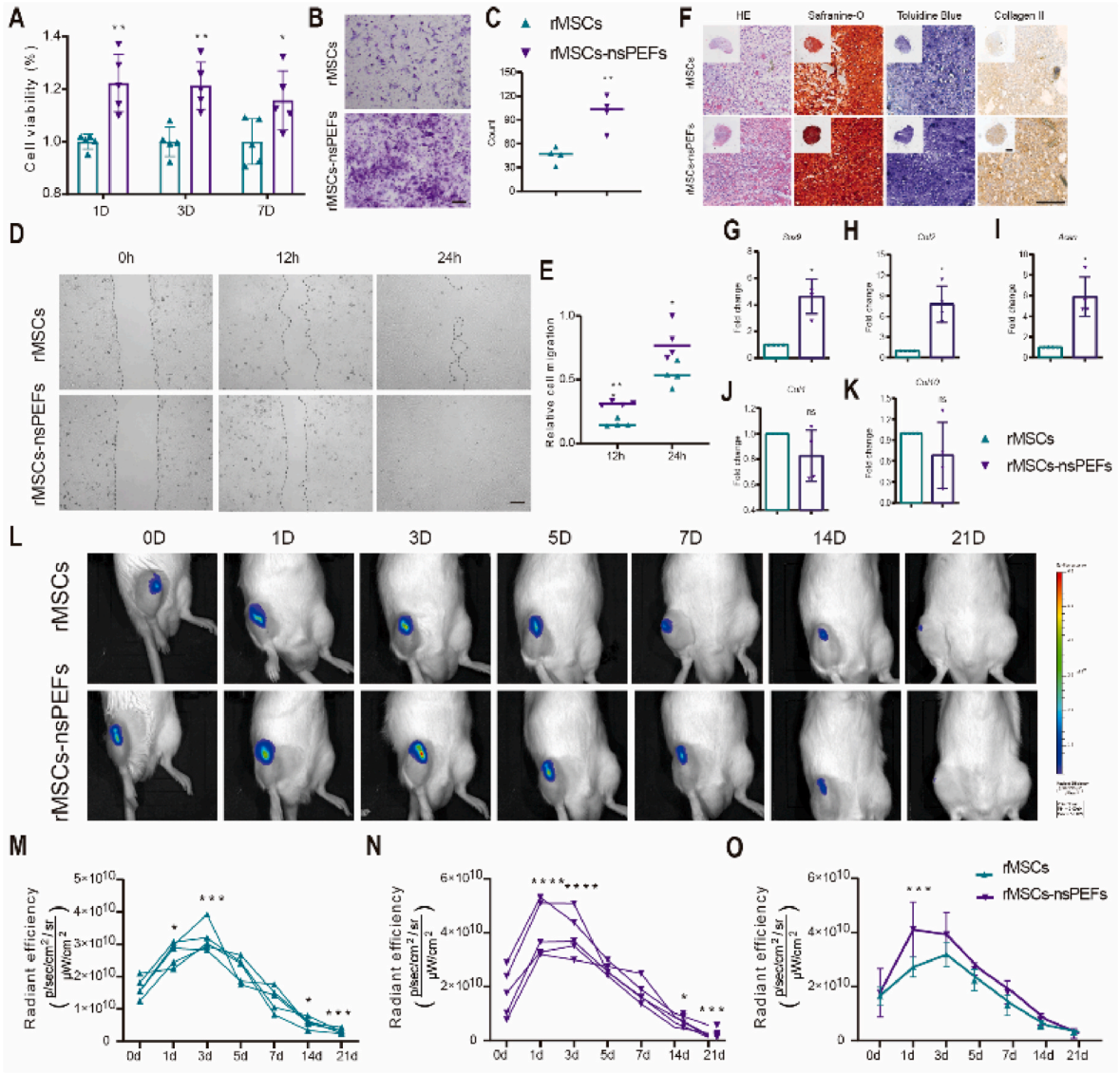

Figure 1. Pretreatment with nsPEFs enhanced viability, migration, chondrogenic differentiation and proliferation of rMSCs. (A) CCK8 assay to determine the viability of rMSCs after nsPEFs treatment (n = 5). (B) Representative images of transwell migration assay of rMSCs-nsPEFs and rMSCs. Scale bars, 100 μm. (C) Quantitative analysis of migrated cells by transwell assay (n = 4). (D) Representative images of scratch test of rMSCs-nsPEFs and rMSCs. Scale bars, 200 μm. (E) Quantitative analysis of cell migration rate (n = 4). (F) Representative images of histological (H&E, Safranine O and Toluidine Blue staining) and immunohistochemistry (collagen II) analysis of rMSCs and rMSCs-nsPEFs pellet (Scale bars, 200 μm). RT-qPCR analysis of chondrogenic genes (G)Sox9, (H) Col2, (I)Acan, (J)Col1, (K)Col10 in pellets of rMSCs and rMSCs-nsPEFs (n = 4). (L) Representative bioluminescence images for tracking *in vivo* cell retention for rMSCs-nsPEFs and rMSCs on days 0, 1, 3, 5, 7, 14 and 21. (M−O) Quantitative analysis of average radiance in standardized regions of interest from rMSCs-nsPEFs and rMSCs injected into the articular cavity of rats. Luminescence signal is presented as photons per second per square centimeter per steradian (n = 5). $^{*}P < 0.05$, $^{**}P < 0.01$, $^{***}P < 0.001$, $^{****}P < 0.0001$.

compared to the control group (wild-type rMSCs), as well as no significant changes in fibrogenesis and hyertrophic markers of *Col1* ($p = 0.1126$) and *Col10 (*$p = 0.5804$)* (Fig. 1F). Similar results in the gene expression of hMSCs (Fig.S2F in Supporting Information) were evidenced. Additionally, biofluorescence imaging showed that the fluorescence of DiR-rMSCs and DiR-rMSCs-nsPEFs in the joint cavity began to increase on day 1 and stabilized on day 3, while decreased significantly on day 14 and basically disappeared on day 21. The fluorescence of DiR-rMSCs-nsPEFs significantly enhanced on the first day compared with DiR-rMSCs, indicating that the proliferation of rMSCs *in vivo* was enhanced Fig. 1L–O). Taken together, these results indicated that nsPEFs pretreatment could improve the viability, migration, chondrogenic differentiation and proliferation of MSCs.

3.2. nsPEFs preconditioned MSCs reversed the change of cartilage markers in OA-like chondrocytes

In order to evaluate the effect of nsPEFs pretreatment on the therapeutic effect of MSCs, co-culture system was used to treat the OA-like chondrocytes which were induced by IL-1β *in vitro* (Fig. 2A). Immunofluorescence analysis showed that IL-1β significantly reduced the expression of Collagen II protein ($p < 0.001$) and increased the level of MMP13 ($p = 0.001$). Co-culture with rMSCs or rMSCs-nsPEFs reversed the effects of IL-1β on Collagen II and MMP13, and these beneficial effects were more significant in the rMSCs-nsPEFs group ($p = 0.0165$) (Fig. 2B and C).

3.3. nsPEFs preconditioned MSCs alleviated pain-related animal behaviors

The therapeutic effects of nsPEFs preconditioned MSCs were evaluated in the ACLT-induced rat OA model with twice joint injection. Gait analysis (Catwalk) can be used to assess pain-related behaviors in rats [26]. We used the catwalk system to collect the gait data of rats before and after ACLT surgery (Fig. 3A). Gait loss was showed in the representative signal image of gait at 1 day after ACLT which is a classic method for animal OA modeling (Fig. 3B). Quantitative data showed that at 1 and 7 days after ACLT surgery, print area, swing speed and duty cycle of RH/LH were significantly reduced, while mean intensity was significantly reduced at the 7 days. All gait parameters returned to normal at 14 days (Fig. 3C–F).

We observed the gait of rats from 1 week to 12 weeks after MSCs treatment (Fig. 3G). Quantitative results showed that rMSCs-nsPEFs increased print area at 1, 4 and 8 weeks after treatment (Fig. 3H). There was no statistically significant difference in swing speed, mean intensity and duty cycle of the right hind paw between the 1–12 weeks after treatment (Fig.S3A-C in Supporting Information). These data indicated that intra-articular injection of rMSCs-nsPEFs can partially relieve pain-related behaviors.

3.4. nsPEFs preconditioned MSCs alleviated structural degeneration **and** reversed the change of cartilage markers in OA

OA is characterized by critical alterations of the subchondral bone microstructure, besides the well-known cartilaginous changes [27]. Micro-CT was used to demonstrate the topography of subchondral bone

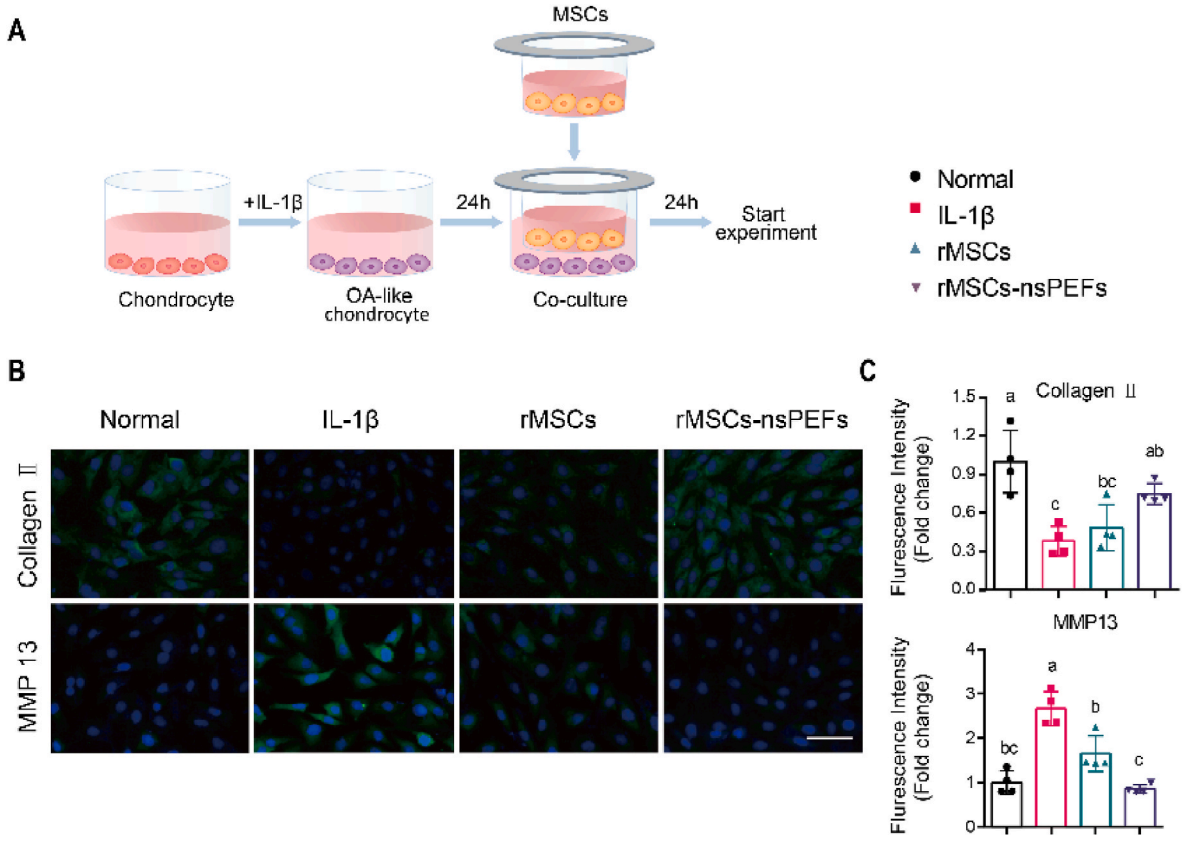

Figure 2. nsPEFs preconditioned rMSCs reversed the change of cartilage markers in OA-like chondrocytes. (A) Schematic diagram of experimental design. (B) Representative images of immunofluorescence assay to detect the expression of Collagen II and MMP13 in chondrocytes in control (Group Normal), OA-like chondrocytes (Group IL-1β), OA-like chondrocytes co-cultured with rMSCs (Group rMSCs) or rMSCs-nsPEFs (Group rMSCs-nsPEFs). Scale bars, 50 μm. (C) Quantitative analysis of immunofluorescence assay to detect the expression of Collagen II and MMP13 in chondrocytes ($n = 4$). Bar labeled with different lowercase letters indicate a significant difference.

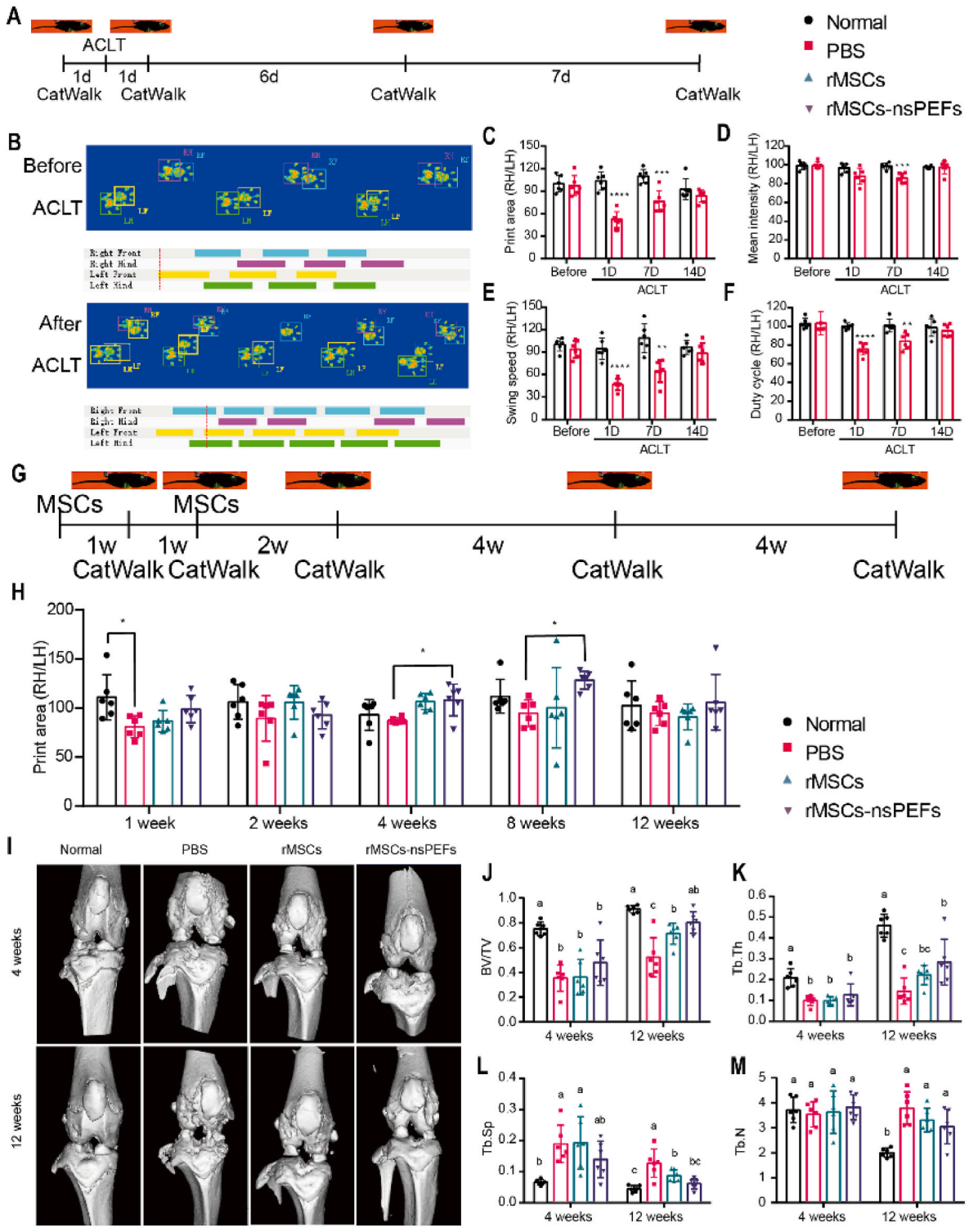

Figure 3. nsPEFs preconditioned rMSCs alleviated pain-related animal behaviors and alleviated subchondral bone changes in OA. (A) Schematic diagram of Catwalk design before and after ACLT surgery. (B) Representative images of Catwalk footprints detected before and after ACLT surgery. The colored bands represent standing time of each foot. (C–F) Analysis changes of gait parameters of print area, mean intensity, swing speed and duty cycle compared among groups before and after ACLT surgery (n = 6). Values are presented as the ratio of the right hind (RH, ACLT applied knee)/the left hind (LH, contralateral knee). (G) Schematic diagram of Catwalk design after rMSCs injection. (H) Analysis changes of gait parameters of print area, compared among groups after rMSCs injection (n = 6). Values are presented as the ratio of the right hind (RH, ACLT applied knee)/the left hind (LH, contralateral knee). (I) Representative images of micro-CT scan and 3D reconstruction of each group of knee joints. Analysis changes of subchondral bone parameters of (J) BV/TV, (K) Tb.Th, (L) Tb.Sp and (M) Tb.N of medial tibial plateau among groups after rMSCs injection (n = 6). Bar labeled with different lowercase letters indicate a significant difference. *$P < 0.05$, **$P < 0.01$, ***$P < 0.001$, ****$P < 0.0001$.

(Fig. 3I–M). At the 4th and 12th week after treatment, the osteophytes formation around the joints in the PBS group was significantly increased, while the articular surface of the rMSCs and rMSCs-nsPEFs treatment groups was smooth with decreased osteophytes formation. Specially, the osteophytes formation was the least in rMSCs-nsPEFs group along all groups (Fig. 3I). Besides, Micro-CT analysis showed that the injection of rMSCs and rMSCs-nsPEFs can also increase tibial trabecular bone volume (BV/TV) ($p = 0.0342$ and $p = 0.008$ respectively) and reduce trabecular bone separation (Tb.Sp) ($p = 0.016$ and $p = 0.003$ respectively) at 12 weeks. In addition, rMSCs-nsPEFs can also significantly reduce the trabecular separation (Tb.Th) at 12 weeks. All these data indicated that rMSCs and rMSCs-nsPEFs can prevent the pathological changes of subchondral bone in the development of OA for a long time, in which the effect of rMSCs-nsPEFs was more significant (Fig. 3J–M).

Articular cartilage defects are potentially severe pathologies that might be involved in the development of OA [28,29]. Histological staining showed that at 4 weeks after treatment, the cartilage in the PBS group was severely degenerated, significantly thinner and the safranin staining became lighter. In contrast, in the rMSCs and rMSCs-nsPEFs groups, cartilage degeneration was slight and safranin staining was slightly lighter (Fig. 4A). At the 12 weeks after treatment, severe diffuse cartilage damage occurred in the PBS group without intact cartilage. At the same time, the cartilage surface was also exfoliated in the rMSCs group. Interestingly, the cartilage in the rMSCs-nsPEFs group was still intact (Fig. 4A).

In order to further study the effect of rMSCs-nsPEFs on the cartilage matrix after ACLT in rats, we performed immunohistochemical staining to determine the expression of Collagen II and MMP13. Immunohistochemical results showed that, the rMSCs and rMSCs-nsPEFs can reverse the reduction of collagen II positive chondrocytes showed in the PBS group at 4 weeks. But the effect of rMSCs cannot sustained for 12 weeks, as there was no difference between the expression of collagen II in the rMSCs group and the PBS group at 12 weeks. However, the rMSCs-nsPEFs can continue to work (Fig. 4B). The Mankin score was used to investigate the degradation level of the articular cartilage by assessing four parameters including: cartilage structure, cellularity, proteoglycan depletion and tidemark integrity. And the heat map showed the score of four parameters, which indicated that rMSCs-nsPEFs had better effect on preventing OA (Fig. 4C–F). Furthermore, compared with the control group, the percentage of MMP13 positive cells increased significantly at 4 weeks (94.04%) and 12 weeks (92.08%) in the PBS group, but not in rMSCs (74.67% at 4 weeks and 67.33% at 12 weeks) and rMSCs-nsPEFs (84.53% at 4 weeks and 70.73% at 12 weeks) groups (Fig. 4G and H). In short, intra-articular injection of rMSCs-nsPEFs reduced the change of cartilage matrix and reduced the destruction of cartilage caused by ACLT.

3.5. RNA-sequence analysis of rMSCs-nsPEFs and rMSCs

RNA Sequencing of MSCs with or without nsPEFs pretreatment was conducted to make a more comprehensive analysis of nsPEFs. We identified 16412 genes, including 116 differentially expressed genes (DEGs, p value < 0.05, $|\log_2(\text{fold change})| > 1$) with 62 upregulated

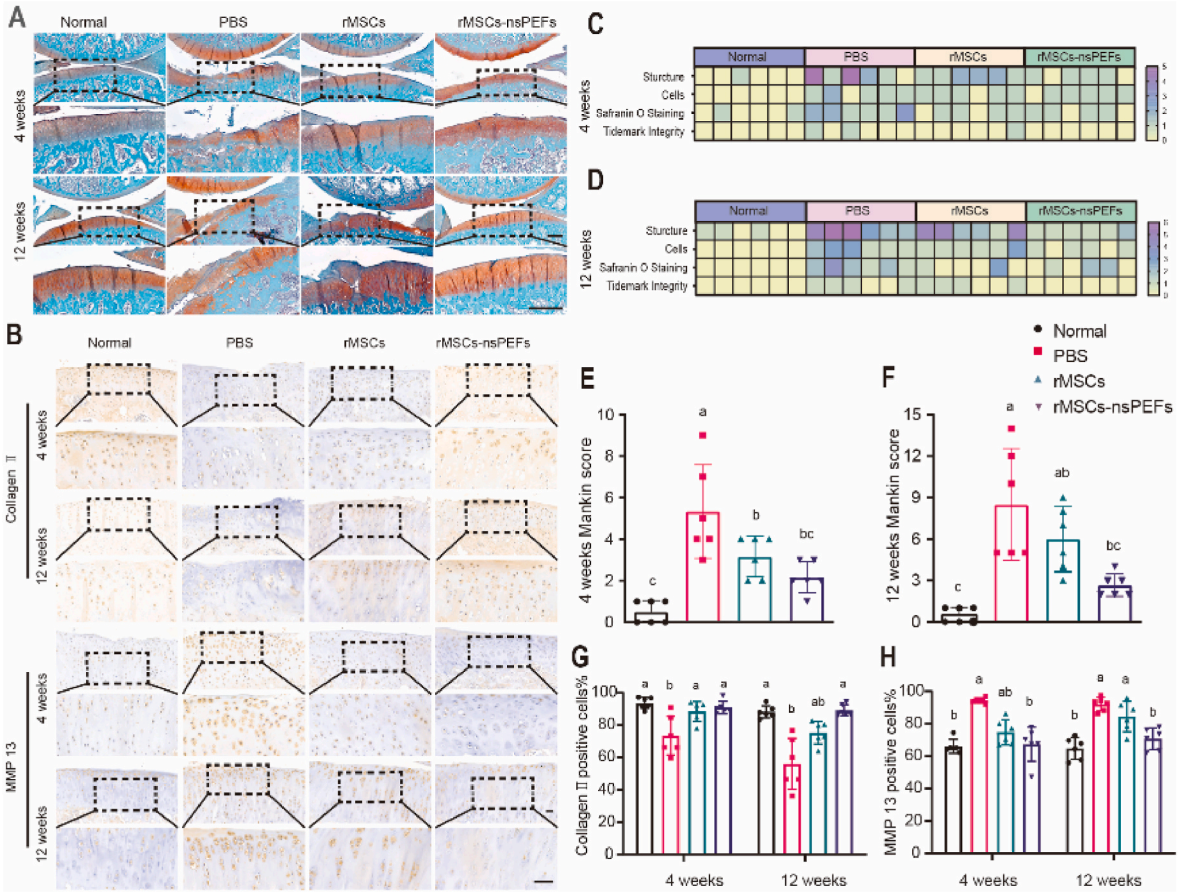

Figure 4. nsPEFs preconditioned MSCs alleviated cartilage changes and reversed the change of cartilage markers in OA rat. (A) Representative images of Safranin O-Fast Green staining of knee joint sections. Scale bars, 500 μm. (B) Representative images of immunohistochemical analysis of Collagen II and MMP13 of knee joint sections. Scale bars, 50 μm. (C) Heat map of variables of the Mankin scoring system at 4 weeks. (D) Heat map of variables of the Mankin scoring system at 12 weeks. (E–F) Analysis changes of cartilage destruction using the Mankin scoring system (n = 6). (G–H) Analysis changes of positive cells of Collagen II and MMP13 in cartilage (n = 6). Bar labeled with different lowercase letters indicate a significant difference.

genes and 49 downregulated genes, in which 30 genes expressed and 18 genes didn't express after nsPEFs pretreatment (Fig. 5A). The heat map was drawn to compare differentially expressed genes in the rMSCs-nsPEFs and rMSCs (Fig. 5B). GO analysis of BP showed that nsPEFs can regulate the chondrogenic differentiation of MSCs (Fig. 5C). Moreover, GO analysis of CC, MF and KEGG pathway analyses of DEGs indicated that nsPEFs can promote paracrine and transmembrane transport of rMSCs (Fig. 5C and D). Therefore, we inferred that nsPEFs not only affected the chondrogenic differentiation, migration and viability of MSCs, but also greatly enhanced the paracrine function of MSCs.

We extracted and analyzed the EVs released from MSCs with or without nsPEFs pretreatment. EVs from rMSCs and rMSCs-nsPEFs were analyzed by TEM, NTA, BCA and western blot analysis. TEM and NTA showed that the morphology and particle size distribution of EVs were similar in the rMSCs and rMSCs-nsPEFs groups (Fig. 6A–C). However, nsPEFs pretreatment significantly increased the number of EVs particles ($p = 0.0154$, and $p = 0.0117$) (Fig. 6B–D). Besides, the EVs protein content of rMSCs-nsPEFs was significantly increased for 5.77 ± 0.92 folds (Fig. 6E, $p = 0.002$). We further detected the protein levels of EVs marker CD9, Alix, TSG101 and endoplasmic reticulum marker Calnexin in the rMSCs-EVs and rMSCs-nsPEFs-EVs. The data showed that the protein levels of CD9, Alix and TSG101 were upregulated in EVs-nsPEFs compared with EVs (Fig. 6F). In summary, these results suggested that

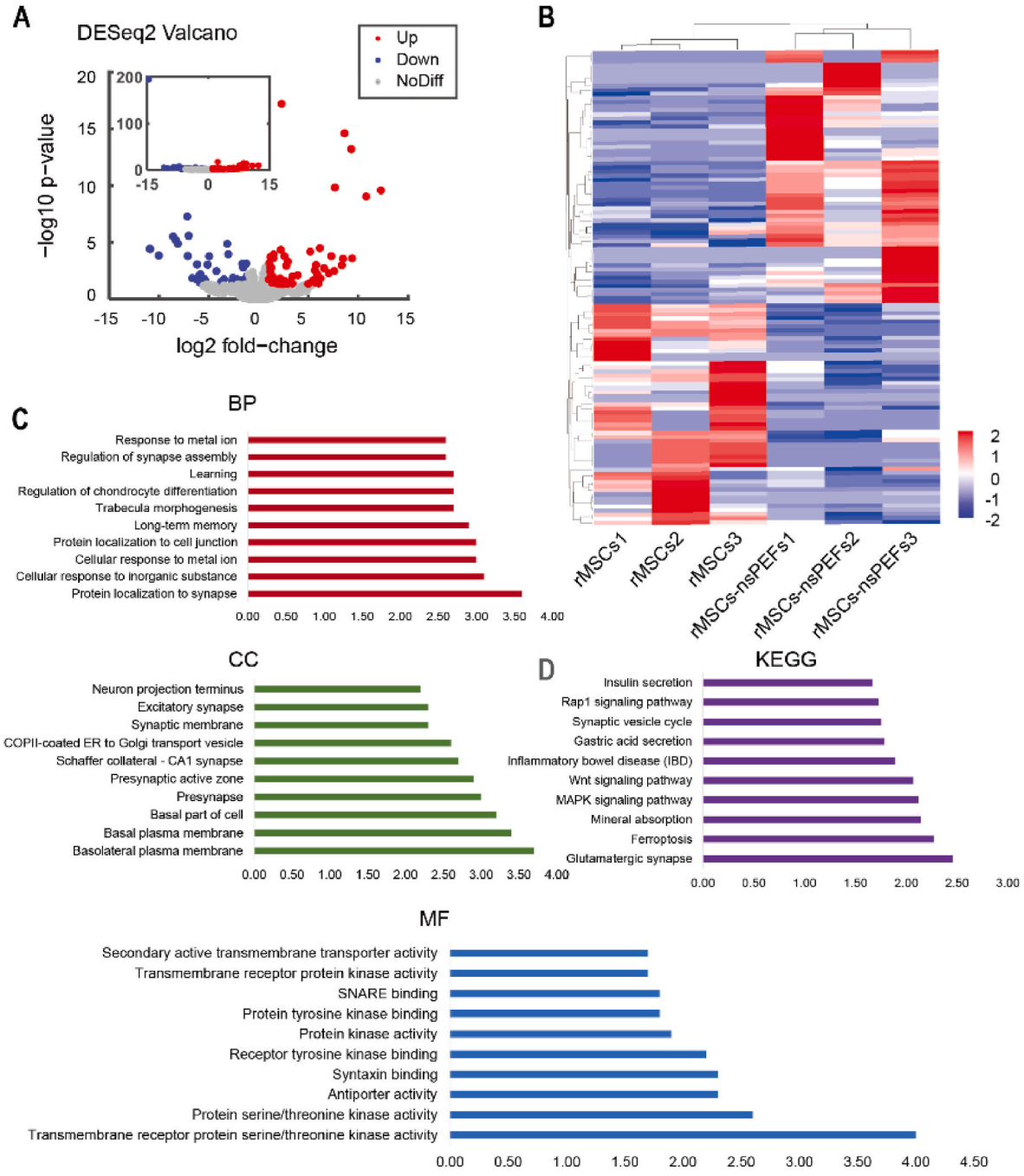

Figure 5. RNA-sequence analysis of rMSCs-nsPEFs and rMSCs. (A) Volcano plot for mRNA expression of MSCs and MSCs-nsPEFs (n = 3). (B) Heatmap of differentially expressed genes (DEGs) with cluster analysis. (C) The top 10 enriched gene ontology terms of DEGs involved in BP, CC, MF. (D) KEGG pathway analysis of DEGs. DEGs, *P* value < 0.05, |log2(fold change) | > 1.

nsPEFs pretreatment can significantly promote the release of EVs.

3.6. EVs-nsPEFs enhanced viability, proliferation, and migration of chondrocytes

To investigate the alteration of EVs properties released from rMSCs-nsPEFs, Dil-labeled EVs and EVs-nsPEFs were co-cultured with chondrocytes. We observed the amounts of EVs and EVs-nsPEFs labeled in red around the nuclei of chondrocytes at 6 h were low, while the uptake of EVs and EVs-nsPEFs by chondrocytes was significantly increased at 12 h and 24 h (Fig. 6G). We assessed the viability of chondrocytes co-cultured with EVs and EVs-nsPEFs with CCK-8 at 1, 3 and 7 days. The results showed that EVs did not enhance the viability of chondrocytes, while EVs-nsPEFs significantly increased the viability of chondrocytes up to 7 days (Fig. 6H, $p = 0.029$). In addition, the results of EDU staining revealed that compared to the PBS group, the number of EDU-stained chondrocytes increased in the EVs ($p = 0.0011$) and EVs-nsPEFs ($p < 0.0001$) groups. However, EVs-nsPEFs administration caused a higher increase in the count of cells stained by EDU (Fig. 6I–K). The migration of chondrocytes co-cultured with EVs and EVs-nsPEFs were detected with the transwell assay. Transwell assay showed that relative to the PBS group, both EVs and EVs-nsPEFs contributed to the migration of chondrocytes. However, compared to EVs alone, EVs-nsPEFs treatment could greatly enhance the migration ability of chondrocytes (Fig. 6J, L, $p = 0.001$).

In order to evaluate the effect of EVs-nsPEFs on the therapeutic effect of OA, co-culture system was used to treat the OA-like chondrocytes which were induced by IL-1β *in vitro* (Fig. 6M and N). Immunofluorescence analysis showed that IL-1β significantly reduced the expression of Collagen II protein and increased the level of MMP13. Co-culture with EVs or EVs-nsPEFs reversed the effects of IL-1β on Collagen II and MMP13, and these beneficial effects were more significant in the EVs-nsPEFs group ($p = 0.0231$ and $p < 0.001$) (Fig. 6O and P). Taken together, these results indicated that EVs-nsPEFs could improve the viability, proliferation, and migration of chondrocytes and reversed the change of cartilage markers.

4. Discussion

PEFs of varying duration and intensity can have different biomedical effects on cells, suggesting a window effect between external PEFs and biological cells [30]. Since nsPEFs do not exist in natural cellular environments, a comprehensive understanding of nsPEF is needed. The effect of nsPEF may depend on several parameters, such as depth, dose, cell type, cell attachment, and tissue type [15]. nsPEFs above 10 kV/cm can cause a series of cell reactions that differ from the electroporation effect. This nsPEF allows perforation of the organelles membrane (inner membrane) such as nucleus and mitochondria without losing the integrity of the outer membrane and may induce apoptosis of tumor cells [30]. Previous study found Tca8113 cells showing early apoptosis after nsPEFs (60 ns, 20 kV/cm, 1 Hz, 20 pulses) combining with radiotherapy [21]. Zhang found that pretreatment of nsPEFs (100 ns, 10 kV/cm or 20 kV/cm, 1 Hz, 5 pulses) can enhance proliferation of chondrocyte [15]. So we think 5 pulses are safe for cells. To optimize experimental parameters, Ning systematically evaluated the cytotoxic effects of nsPEFs with 16 conditions (4 durations with 4 field strength) on MSCs. Remarkably, high field strength or long duration can lead to apoptosis or reduced cell viability, whereas nsPEFs at a lower intensity of 5 kV/cm exhibited minimal cytotoxic effects, even with increased exposure times [18]. So we chose the right field strength and duration as the stimulus parameter for MSCs. We previously found that nsPEFs (100 ns, 10 kV/cm, 1 Hz, 5 pulses) can improve the stemness of porcine bone marrow MSCs (pMSCs), hMSCs and rMSCs, and promote the osteochondral defect repair of rats [16,18,22]. Here, we further found that nsPEFs with the same parameters can improve the migration, viability and EVs release of rMSCs and hMSCs, and enhance rMSCs therapeutic effect on OA-like chondrocytes induced by IL-1β *in vitro* and ACLT-induced OA rat model *in vivo*. Our results suggested that the nsPEFs we used can improve the cell therapy capabilities of MSCs with multi-target.

nsPEFs pretreatment temporarily enhanced the proliferation of MSCs *in vivo*. In details, the radiant efficiency was significantly higher in nsPEFs-MSCs group compared with which in MSCs group on the first day after injection, and the higher radiant efficiency can last for 14 days, although there was no significant difference subsequently. While the promoting effect of nsPEFs on the proliferation of MSCs was still unable to resist the elimination of MSCs, as the residence time of MSCs with or without nsPEFs pretreatment both reduced sharply at 14 days and disappeared at 21 days, which is consistent with the previous findings of Wang et al. [31]. Our previous studies have shown that a single injection of MSCs can temporarily slow the progression of cartilage degradation in a rat OA model, but its long-term therapeutic effect is limited [32] , while multiple injections of MSCs can slow down the progression of OA for a long time [33]. Combining MSCs and scaffold materials can increase the residence time of MSCs in the joint cavity [31,34]. We suspected that the promoting effect of nsPEFs on the proliferation of MSCs can be further amplified by the scaffold material, and the combination of nsPEFs and scaffold material may further increase the residence time of MSCs in the joint cavity.

MSCs pretreated with nsPEFs have a significant effect on the treatment of OA. Through imaging and histological staining analysis, we found that compared with PBS and rMSCs injection, rMSCs-nsPEFs achieved a considerable repair effect in the rat OA model, which was consistent with the results *in vitro*. Particularly, the nsPEFs pretreatment can be applied in 10 s, which means that nsPEFs can be an efficient and fast method for MSCs stimulation on OA clinical treatment. On the other hand, we had found that nsPEFs can increase the sensitivity of MSCs to other factors [17]. Therefore, nsPEFs can be combined with other factors to further inhibit the process of OA and promote cartilage regeneration.

The pretreatment of MSCs with nsPEFs significantly alleviated the pain of OA rats. Gait analysis has become a crucial method for measuring OA pain. Zhang et al.'s study demonstrated a significant reduction in the duty cycle of the injured right hind paw 1 day and 1 week after DMM, returning to normal 2 weeks post-operation [35], consistent with our study's results within 2 weeks after ACLT. Previous research showed that gait parameters remained unchanged at 8 weeks after DMM but were significantly reduced at 12 weeks after DMM [36]. Wu et al. found that the decrease in duty cycle could be reversed by intra-articular injection of MSC-EVs at 10 weeks after DMM [5], with similar but not identical results to our current research. Our study showed a significant improvement in the print area of the right hind paw of rats at 1 week, 4 weeks, and 8 weeks after intra-articular injection of rMSCs-nsPEFs, with no obvious changes in other time points and gait parameters. Continuous video tracking of the trajectory of the hind paw of OA mice revealed significant changes in gait characteristics after 1–14 weeks after DMM, including some gait indexes of the left hind paw (unpublished results). In addition, the previous research of our research group found that after the treatment of human umbilical cord-derived mesenchymal stem cells (hUC-MSCs) in rats after ALCT + medial meniscectomy, the pain behavior of rats was not improved. Therefore, regenerative therapy (such as MSCs injection) combined with pharmacological therapies to target pain may achieve substantial therapeutic effects in the treatment of OA [32]. For example, combination of magnesium ions and vitamin C alleviates significantly improved the gait changes of OA mice at different time points in the study of Yao et al. [26].

nsPEFs promote the release of EVs from MSCs and EVs-nsPEFs enhanced viability, proliferation and migration of chondrocytes and reversed the change of cartilage markers in OA-like chondrocytes. MSCs-EVs have important therapeutic effects and are a research hotspot in the field of tissue regeneration currently. However, the very low yield of EVs limits its application [37], and many studies are devoted to improving

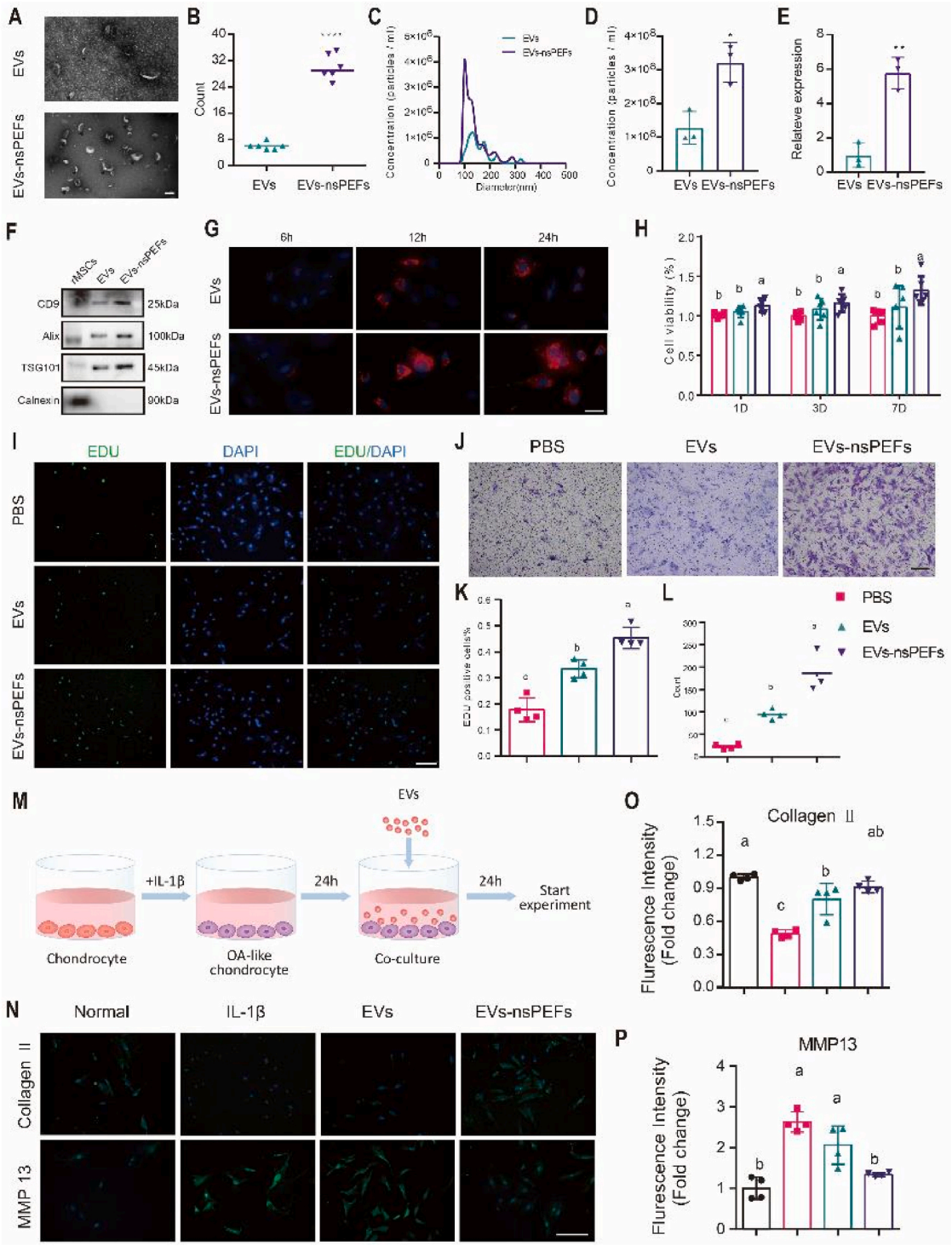

Figure 6. nsPEFs enhanced the release of EVs from MSCs and EVs-nsPEFs enhanced viability, proliferation and migration of chondrocytes and reversed the change of cartilage markers in OA-like chondrocytes. (A) Morphology of EVs and EVs-nsPEFs under TEM. Scale bars, 200 nm. (B) The number of EVs in random field (n = 6) was counted. (C) EVs size distributions and particle concentration analyzed by NTA. (D) Analysis changes of particle concentration between EVs and EVs-nsPEFs. (E) Analysis changes of the protein concentration between EVs and EVs-nsPEFs using BCA method. (F) WB results for the EVs markers CD9, Alix, TSG101 and the negative marker Calnexin. (G) Representative bioluminescence images for Red dye Dil-labeled EVs and EVs-nsPEFs in chondrocytes at 6 h, 12 h and 24 h. Scale bars, 50 μm. (H) CCK8 assay to determine the viability of chondrocytes co-cultured with EVs and EVs-nsPEFs (n = 6). (I) Representative images of EDU staining of chondrocytes co-cultured with EVs and EVs-nsPEFs. Scale bars, 200 μm. (J) Representative images of transwell migration assay of chondrocytes co-cultured with EVs and EVs-nsPEFs. Scale bars, 100 μm. (K) Quantitative analysis of positive cells by EDU staining (n = 4). (L) Quantitative analysis of migrated cells by transwell assay (n = 4). (M) Schematic diagram of experimental design. (N) Representative images of immunofluorescence assay to detect the expression of Collagen II and MMP13 in chondrocytes in control (Group Normal), OA-like chondrocytes (Group IL-1β), OA-like chondrocytes co-cultured with EVs (Group EVs) or EVs-nsPEFs (Group EVs-nsPEFs). Scale bars, 50 μm. Quantitative analysis of immunofluorescence assay to detect the expression of (O) Collagen II and (P) MMP13 in chondrocytes (n = 4). $^{*}P < 0.05$, $^{**}P < 0.01$, $^{****}P < 0.0001$. Bar labeled with different lowercase letters indicate a significant difference.

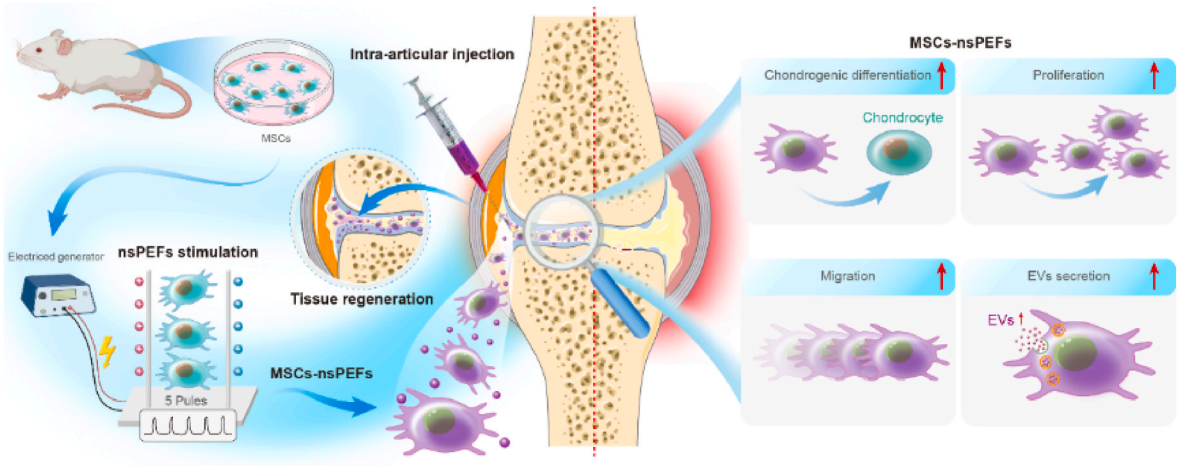

Figure 7. Schematic illustration for the role of nsPEFs in the MSCs-based OA therapy.

the yield of EVs, such as genetic modification [38], chemical [39] and physical factor [40] induction. Here, with only 5 electrical pulses stimulation, the secretion of EVs can be significantly increased, where the number of particles increased by more than 3 folds, and the protein content improved by nearly 6 folds. In additional, nsPEFs treatment could improve the performance of MSCs-EVs and the ability to hinder OA. These results manifested that nsPEFs have great clinical application value in regulating the secretion of EVs. In mechanism, study had shown that increased intracellular calcium ion caused by electrical stimulation can promote the release of EVs from cells [41]. In this study, nsPEFs can activate calcium ion channels, which is in line with the other research [42]. So nsPEFs may also promote the release of EVs through calcium ion channels which needed to be explored in deeply in the future. Moreover, nsPEFs treatment changing the composition of MSCs-EVs is also worth studying, we will focus on this point by micro-RNA sequencing to study the changes of EVs and to provide a more solid theoretical basis for clinical applications [43].

There are still some limitations in our current research. First of all, in order to ensure the therapeutic effect, we repeatedly inject rMSCs, which poses a certain risk of infection. The member of our research group have developed an injectable three-dimensional microcryogel as a cell delivery vehicle, which has been proven to improve the residence time of MSCs in the joint cavity of rats and the therapeutic effect of OA [31,34]. In our future studies of MSCs-nsPEFs in the treatment of OA, MSCs-nsPEFs will be combined with the microcryogel to reduce the frequency of MSCs injection. Secondly, we conducted *in vivo* study with rats. There is still a certain gap between this small rodent model with humans. The arrangement of collagen fibers in pig articular cartilage is very similar to the leaf-like arrangement of humans [44]. Miniature pigs have the characteristics of large joint size, thick articular cartilage layer and fully extended and erect knee joints during gait. They are very similar to the anatomical structure and physiological characteristics of human knee joints. In addition, adult miniature pigs usually grow to adult weight (70 kg), which can provide realistic body load and more closely imitated the human environment [45].Therefore, before determining the clinical relevance of MSCs preated with nsPEFs to treat OA, it is necessary to conduct research in larger animals such as miniature pigs.

In summary, the pretreatment of nsPEFs exhibits a profound impact on augmenting the cellular functionality of MSCs, encompassing their differentiation, migration, viability, and EVs secretion. Notably, the nsPEF-pretreated MSCs effectively suppress the progression of OA both *in vitro* and *in vivo*, as depicted in Fig. 7. Considering the swift application time of only 10 s for nsPEFs pretreatment, this approach holds great promise as a highly effective method to optimize the therapeutic efficacy of MSCs and EVs.

5. Conclusions

nsPEFs pretreatment can significantly enhance the cell performance of MSCs, including the differentiation, migration, viability and EVs secretion. Particularly, MSCs pretreated by nsPEFs greatly inhibited the development of OA *in vitro* and *in vivo*. Regarding that nsPEFs pretreatment can be applied in 10 s, it will be a promising and effective method to optimize the therapeutic effect of MSCs.

Funding

This study was funded by grants from the National Natural Science Foundation of China (81902247, 81672183, 81772334), National Key Research and Development Program of China (2020YFC2004900, 2020YFC2004904), Guangdong Basic and Applied Basic Research Foundation (2022A1515220056), Beijing Municipal Science & Technology Commission (7232097) and Beijing Natural Science Foundation (L212044).

Ethics approval

This study was in accordance with the Declaration of Helsinki. All experiments were performed in accordance with the guidelines and ethical procedures of Peking University and Peking University People's Hospital. All procedures of animal usage were approved by the Institutional Animal Care and Use Committee of Peking University (approval number: COE-GeZ-7; date of approval: July 23, 2021). All adult human MSCs were obtained, with approval of the Ethics Review Committee of Peking University People's Hospital (approval number: 2018PHC061; date of approval: May 28, 2019).

Availability of data and materials

The datasets used and/or analyzed during the current study are available from the corresponding author on reasonable request.

Consent for publication

All authors agree to publish this manuscript.

Credit authors statement

JL (Jianjing Lin): Experiment implementation, Data analysis, Manuscript Writing. KL: Experiment implementation, Data analysis, Manuscript Writing. ZY: Experiment implementation, Manuscript Writing. FC: Experiment implementation. LG: Data analysis. TN: Data

analysis. DX: Data analysis. HZ: Conception and design. QL: Conception and design. ZG: Conception and design, Writing - review & editing, Supervision. JL (Jianhao Lin): Conception and design, Writing - review & editing, Supervision.

Declaration of competing interest

The authors declare that there are no conflicts of interest.

Abbreviations

ACLT	anterior cruciate ligament transection
BSA	bovine serum albumin
BV/TV	bone volume/total tissue volume
CCK-8	cell counting kit-8
DEGs	differentially expressed genes
DMEM	dulbecco's modified eagle's medium
DMM	destabilization of medial meniscus
EVs	extracellular vesicles
FBS	fetal bovine serum
GAPDH	glyceraldehyde-3-phosphate dehydrogenase
H&E	haematoxylin and eosin
hMSCs	human bone marrow mesenchymal stem cells
hUC-MSCs	human umbilical cord-derived mesenchymal stem cells
MSCs	mesenchymal stem cells
MSCs-nsPEFs	MSCs preteated with nsPEFs
NTA	nanoparticle tracking analysis
OA	osteoarthritis
PEFs	pulsed electric fields
pMSCs	porcine bone marrow mesenchymal stem cells
PS	penicillin/streptomycin
rMSCs	rat bone marrow mesenchymal stem cells
ROI	region of interest
SDS	sodium dodecyl sulfate
Tb.Sp	trabecular separation
Tb.Th	trabecular thickness
Tb.N	trabecular number
TEM	transmission electron microscopy
nsPEFs	nanosecond pulsed electric fields

Appendix A. Supplementary data

Supplementary data to this article can be found online at https://doi.org/10.1016/j.jot.2024.03.006.

References

[1] Hunter DJ, March L, Chew M. Osteoarthritis in 2020 and beyond: a Lancet commission. Lancet 2020;396(10264):1711–2.
[2] Gao L, Han Z, Xiong A. Total hip arthroplasty or hemiarthroplasty for hip fracture. N Engl J Med 2020;382:1072–3.
[3] Kalamegam G, Memic A, Budd E, Abbas M, Mobasheri A. A comprehensive review of stem cells for cartilage regeneration in osteoarthritis. Adv Exp Med Biol 2018;1089:23–36.
[4] Lamo-Espinosa JM, Blanco JF, Sánchez M, Moreno V, Granero-Moltó F, Sánchez-Guijo F, et al. Phase II multicenter randomized controlled clinical trial on the efficacy of intra-articular injection of autologous bone marrow mesenchymal stem cells with platelet rich plasma for the treatment of knee osteoarthritis. J Transl Med 2020;18(1):356.
[5] Wu J, Kuang L, Chen C, Yang J, Zeng WN, Li T, et al. miR-100-5p-abundant exosomes derived from infrapatellar fat pad MSCs protect articular cartilage and ameliorate gait abnormalities via inhibition of mTOR in osteoarthritis. Biomaterials 2019;206:87–100.
[6] Jiang S, Tian G, Li X, Yang Z, Wang F, Tian Z, et al. Research progress on stem cell therapies for articular cartilage regeneration. Stem Cell Int 2021;2021:8882505.
[7] Hu C, Li L. Preconditioning influences mesenchymal stem cell properties in vitro and in vivo. J Cell Mol Med 2018;22(3):1428–42.
[8] Yin B, Ni J, Witherel CE, Yang M, Burdick JA, Wen C, et al. Harnessing tissue-derived extracellular vesicles for osteoarthritis theranostics. Theranostics 2022;12:207–31.
[9] Ai M, Hotham WE, Pattison LA, Ma Q, Henson F, Smith E. Role of human mesenchymal stem cells and derived extracellular vesicles in reducing sensory neuron hyperexcitability and pain behaviors in murine osteoarthritis. Arthritis Rheumatol 2023;75:352–63.
[10] Bhatti FU, Mehmood A, Latief N, Zahra S, Cho H, Khan SN, et al. Vitamin E protects rat mesenchymal stem cells against hydrogen peroxide-induced oxidative stress in vitro and improves their therapeutic potential in surgically-induced rat model of osteoarthritis. Osteoarthritis Cartilage 2017;25(2):321–31.
[11] Robb KP, Gabrial S, Mirzaesmaeili A, Kapoor M, Audet J, Gandhi R, et al. Desirability profiling to rank mesenchymal stromal cell enhancement methods for osteoarthritis treatment. Osteoarthritis Cartilage 2021;29:S209.
[12] Tanaka E, Liu Y, Xia L, Ogasawara N, Sakamaki T, Kano F, et al. Effectiveness of low-intensity pulsed ultrasound on osteoarthritis of the temporomandibular joint: a review. Ann Biomed Eng 2020;48(8):2158–70.
[13] Guo R, Gao L, Xu B. Current evidence of adult stem cells to enhance anterior cruciate ligament treatment: a systematic review of animal trials. Arthroscopy 2018;34:331–340.e2.
[14] Kim IS, Song JK, Song YM, Cho TH, Lee TH, Lim SS, et al. Novel effect of biphasic electric current on in vitro osteogenesis and cytokine production in human mesenchymal stromal cells. Tissue Eng 2009;15(9):2411–22.
[15] Zhang K, Guo J, Ge Z, Zhang J. Nanosecond pulsed electric fields (nsPEFs) regulate phenotypes of chondrocytes through Wnt/β-catenin signaling pathway. Sci Rep 2014;4:5836.
[16] Li K, Ning T, Wang H, Jiang Y, Zhang J, Ge Z. Nanosecond pulsed electric fields enhance mesenchymal stem cells differentiation via DNMT1-regulated OCT4/NANOG gene expression. Stem Cell Res Ther 2020;11:308.
[17] Li K, Fan L, Lin J, Heng BC, Deng Z, Zheng Q, et al. Nanosecond pulsed electric fields prime mesenchymal stem cells to peptide ghrelin and enhance chondrogenesis and osteochondral defect repair in vivo. Sci China Life Sci 2022;65(5):927–39.
[18] Ning T, Guo J, Zhang K, Li K, Zhang J, Yang Z, et al. Nanosecond pulsed electric fields enhanced chondrogenic potential of mesenchymal stem cells via JNK/CREB-STAT3 signaling pathway. Stem Cell Res Ther 2019;10:45.
[19] Fan L, Chen J, Tao Y, Heng BC, Yu J, Yang Z, et al. Enhancement of the chondrogenic differentiation of mesenchymal stem cells and cartilage repair by ghrelin. J Orthop Res 2019;37(6):1387–97.
[20] Beebe SJ, Schoenbach KH, Heller R. Bioelectric applications for treatment of melanoma. Cancers 2010;2(3):1731–70.
[21] Guo J, Wang Y, Wang J, Zhang J, Fang J. Radiosensitization of oral tongue squamous cell carcinoma by nanosecond pulsed electric fields (nsPEFs). Bioelectrochemistry 2017;113:35–41.
[22] Li K, Fan L, Lin J, Heng BC, Deng Z, Zheng Q, et al. Nanosecond pulsed electric fields prime mesenchymal stem cells to peptide ghrelin and enhance chondrogenesis and osteochondral defect repair in vivo. Sci China Life Sci 2022;65:927–39.
[23] Wang L, Feng Z, Wang X, Wang X, Zhang X. DEGseq: an R package for identifying differentially expressed genes from RNA-seq data. Bioinformatics 2010;26(1):136–8.
[24] Zhou Y, Zhou B, Pache L, Chang M, Khodabakhshi AH, Tanaseichuk O, et al. Metascape provides a biologist-oriented resource for the analysis of systems-level datasets. Nat Commun 2019;10(1):1523.
[25] Bu D, Luo H, Huo P, Wang Z, Zhang S, He Z, et al. KOBAS-i: intelligent prioritization and exploratory visualization of biological functions for gene enrichment analysis. Nucleic Acids Res 2021;49(W1):W317–317W325.
[26] Yao H, Xu J, Wang J, Zhang Y, Zheng N, Yue J, et al. Combination of magnesium ions and vitamin C alleviates synovitis and osteophyte formation in osteoarthritis of mice. Bioact Mater 2021;6(5):1341–52.
[27] Oláh T, Cai X, Gao L, Walter F, Pape D, Cucchiarini M, et al. Quantifying the human subchondral trabecular bone microstructure in osteoarthritis with clinical CT. Adv Sci 2022;9:e2201692.
[28] Cucchiarini M, Madry H. Biomaterial-guided delivery of gene vectors for targeted articular cartilage repair. Nat Rev Rheumatol 2019;15:18–29.
[29] Schrenker S, Cucchiarini M, Goebel L, Oláh T, Venkatesan JK, Schmitt G, et al. In vivo rAAV-mediated human TGF-β overexpression reduces perifocal osteoarthritis and improves osteochondral repair in a large animal model at one year. Osteoarthritis Cartilage 2023;31:467–81.
[30] Yao C, Hu X, Mi Y, Li C, Sun C. Window effect of pulsed electric field on biological cells. IEEE Trans Dielectr Electr Insul 2009;16:1259.
[31] Wang B, Liu W, Li JJ, Chai S, Xing D, Yu H, et al. A low dose cell therapy system for treating osteoarthritis: in vivo study and in vitro mechanistic investigations. Bioact Mater 2022;7:478–90.
[32] Xing D, Wu J, Wang B, Liu W, Liu W, Zhao Y, et al. Intra-articular delivery of umbilical cord-derived mesenchymal stem cells temporarily retard the progression of osteoarthritis in a rat model. Int J Rheum Dis 2020;23(6):778–87.
[33] Xing D, Wang K, Wu J, Zhao Y, Liu W, Li JJ, et al. Clinical-grade human embryonic stem cell-derived mesenchymal stromal cells ameliorate the progression of osteoarthritis in a rat model. Molecules 2021;26(3):604.
[34] Xing D, Liu W, Wang B, Li JJ, Zhao Y, Li H, et al. Intra-articular injection of cell-laden 3D microcryogels empower low-dose cell therapy for osteoarthritis in a rat model. Cell Transplant 2020;29:963689720932142.
[35] Zhang B, Chen H, Ouyang J, Xie Y, Chen L, Tan Q, et al. SQSTM1-dependent autophagic degradation of PKM2 inhibits the production of mature IL1B/IL-1β and contributes to LIPUS-mediated anti-inflammatory effect. Autophagy 2020;16(7):1262–78.
[36] Muramatsu Y, Sasho T, Saito M, Yamaguchi S, Akagi R, Mukoyama S, et al. Preventive effects of hyaluronan from deterioration of gait parameters in surgically induced mice osteoarthritic knee model. Osteoarthritis Cartilage 2014;22(6):831–5.

[37] Gowen A, Shahjin F, Chand S, Odegaard KE, Yelamanchili SV. Mesenchymal stem cell-derived extracellular vesicles: challenges in clinical applications. Front Cell Dev Biol 2020;8:149.
[38] Kojima R, Bojar D, Rizzi G, Hamri GC, El-Baba MD, Saxena P, et al. Designer exosomes produced by implanted cells intracerebrally deliver therapeutic cargo for Parkinson's disease treatment. Nat Commun 2018;9(1):1305.
[39] Liao Z, Li S, Lu S, Liu H, Li G, Ma L, et al. Metformin facilitates mesenchymal stem cell-derived extracellular nanovesicles release and optimizes therapeutic efficacy in intervertebral disc degeneration. Biomaterials 2021;274:120850.
[40] Ullah M, Liu DD, Rai S, Razavi M, Concepcion W, Thakor AS. Pulsed focused ultrasound enhances the therapeutic effect of mesenchymal stromal cell-derived extracellular vesicles in acute kidney injury. Stem Cell Res Ther 2020;11(1):398.
[41] Yang Z, Shi J, Xie J, Wang Y, Sun J, Liu T, et al. Large-scale generation of functional mRNA-encapsulating exosomes via cellular nanoporation. Nat Biomed Eng 2020;4(1):69–83.
[42] Muratori C, Pakhomov AG, Gianulis E, Meads J, Casciola M, Mollica PA, et al. Activation of the phospholipid scramblase TMEM16F by nanosecond pulsed electric fields (nsPEF) facilitates its diverse cytophysiological effects. J Biol Chem 2017;292(47):19381–91.
[43] Gao L, Guo R, Han Z, Liu J, Chen X. Clinical trial reporting. Lancet 2020;396:1488–9.
[44] Kääb MJ, Gwynn IA, Nötzli HP. Collagen fibre arrangement in the tibial plateau articular cartilage of man and other mammalian species. Pt 1 J Anat 1998;193(Pt 1):23–34.
[45] Martin AR, Patel JM, Locke RC, Eby MR, Saleh KS, Davidson MD, et al. Nanofibrous hyaluronic acid scaffolds delivering TGF-β3 and SDF-1α for articular cartilage repair in a large animal model. Acta Biomater 2021;126:170–82.